International Refrigeration and Air Conditioning Conference

School of Mechanical Engineering

2004

Fault Detection Based on Motor Start Transients and Shaft Harmonics Measured at the RTU Electrical Service

Peter R. Armstrong
MIT

Chris R. Laughman
MIT

Steven B/ Leeb
MIT

Leslie K. Norford
MIT

Follow this and additional works at: http://docs.lib.purdue.edu/iracc

FAULT DETECTION BASED ON MOTOR START TRANSIENTS AND SHAFT HARMONICS MEASURED AT THE RTU ELECTRICAL SERVICE

Peter R. Armstrong[1], Chris R. Laughman, Steven B. Leeb, Leslie K. Norford
MIT 5-418, 77 Massachusetts Ave., Cambridge, MA 02139

ABSTRACT

Non-intrusive load monitoring (NILM) is accomplished by sampling voltage and current at high rates and reducing the resulting start transients or harmonic content to concise "signatures." Changes in these signatures can be used to detect, and possibly diagnose, equipment and component faults associated with roof-top cooling units. Use of the NILM for fault detection and diagnosis (FDD) is important because 1) it complements other FDD schemes that are based on thermo-fluid sensors and analyses and 2) it is minimally intrusive (one measuring point in the relatively protected confines of the control panel) and therefore inherently reliable. This paper describes changes in the power signatures of fans and compressors that were found, experimentally and theoretically, to be useful for fault detection.

1. INTRODUCTION

Hardware and control failures represent a large fraction of U.S. HVAC operational costs (Katipamula and Gaines 2003). Comfort and consequent productivity loss may represent significant additional costs. Unitary equipment appears to be just as susceptible to performance degradation as built-up systems (Breuker 1998a). Roof-top unit (RTU) faults often go undetected by occupants and maintenance staff. A "wait for complaints" strategy is often taken in spite of its many well known negative side effects. There are two generally accepted paths to correcting this situation: 1) test-and-measurement-based preventive maintenance[2] and 2) automated on-line fault detection. The key to cost-effective on-line fault detection and diagnosis (FDD) is finding the optimal mix of sensors and automated analysis for a given target system. Much attention has focused on temperature-measurement based fault detection because of low sensor cost (Rossi and Braun 1997). However, temperature sensor location is critical; sensors must be installed in specific locations regardless of the resulting susceptibility to harsh environments or damage during inspection and service activities. Consequently, more expensive but less intrusive sensor types, such as pressure and power, may be justified by improved reliability.

A device called the non-intrusive load monitor (NILM) is extremely well suited to the tasks of measuring and analyzing electrical signals (Leeb 1992, Shaw *et al*. 1998, Laughman *et al*. 2003) that may be useful in fault detection. Results of recent tests, reported here, show that some RTU thermo-fluid faults can be detected by the NILM alone. Certain mechanical (motor and fan) faults and most electrical (supply, controls, motor) faults can also be detected. In this paper, previous research is reviewed, and the responses to faults (artificially introduced in an operating unit) of steady and transient electrical loads are characterized. New methods of detecting bypass leakage, fan imbalance, and liquid ingestion faults are described and fault detection implementation issues are discussed.

2. PREVIOUS RESEARCH

The frequency of faults in unitary cooling equipment has been assessed from substantial insurance claim and service record data bases by Stouppe and Lau (1989) and Breuker and Braun (1998a). Stouppe and Lau (1989) compiled 15,716 failure records and attribute 76% of faults to electrical components, 19% to mechanical and 5% to refrigerant circuit components. Of the electrical failures 87% were motor winding failures from deterioration of insulation (vibration, overheating) unbalanced operation and short cycling (overheating). The reported numbers refer to events; costs of repair were not published. Rossi and Braun (1993) reviewed various detection and diagnostic methods and later (1997) developed effective rule-based methods.

Rossi (1997), Rossi and Braun (1997) and Breuker and Braun (1998a, 1998b) applied detection, diagnosis and evaluation methods and performed statistical analyses of detection sensitivity at specific fault levels. Two prototype

---

[1] Armstrong is on educational leave from PNNL and can be reached at pr_armstrong@pnl.gov 617-452-2286
[2] Including such concepts as re-commissioning or continuous commissioning

systems, designated the low-cost system (2 temperature inputs, 5 outputs) and the high-performance system (3 inputs, 7 outputs), were developed and fault detection (without excessive false alarm rates) was generally found to be effective when capacity and COP dropped by 10 to 20% for five common mechanical faults:

Refrigerant leakage, undercharge or overcharge;
Liquid line restriction;
Loss of volumetric efficiency (leaky valves, seals);
Fouled condenser coil;
Dirty supply air filter.

3. FAULT TESTING AND ANALYSIS

Of the five faults noted above, NILM detection was attempted for all but the liquid-line-restriction fault. Purely electrical faults were not tested. Contact erosion and bounce have already been successfully tested (Shaw 2000). Detection of an unbalanced three-phase voltage condition (failure of any phase to maintain a preset threshold voltage for a preset number of cycles while the other two hold up) is completely straightforward. Two new mechanical faults, rotor imbalance and flooded start/liquid ingestion, were therefore selected for testing. Detection was based on analysis of real (P1) and reactive power (Q1), computed from measurements of voltage and current.

Evaporator and condenser blockage were artificially introduced by inserting strips of cardboard against the heat exchanger inlet face. This achieved a quasi-uniform flow distribution of known blockage factor. Refrigerant over- and undercharge conditions were achieved by evacuating the system, then adding a known mass of refrigerant to obtain the desired level of charge. Leaky valves or seals were mimicked by opening the hot bypass valve a specific amount and making repeated compressor starts. Fan imbalance was artificially introduced by adding small weights of known mass near the rotor tip at one point on the circumference. For the supply fan, binder clips were fastened to a vane from inside the squirrel cage. For the condenser, a known mass was affixed at the tip of one blade.

3.1 Short Cycling

Compressor start transients with no pressure relief between starts and with the fans turned off are shown in Figure 1. The compressor cycling frequency of about three starts per minute is much higher than the shortest cycling frequency of normal operation and is therefore representative of a short-cycling fault. The main difference between start traces is that the final value of P1 (time index >50) increases with successive starts, a phenomenon not seen with pressure relief between starts.
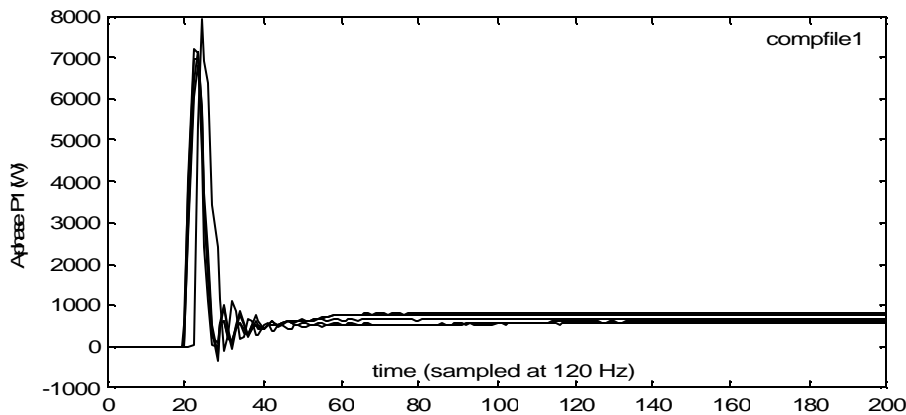

Figure 1. Five compressor starts with no pressure relief.

3.2 Refrigerant Charge

Evaporator and condenser capacity are adversely affected by incorrect refrigerant charge. The system can be overcharged or undercharged. In either case, excessive portions of the evaporator or condenser are relegated to sensible, rather than boiling or condensing, modes of heat transfer. With undercharge there is too much vapor being superheated in the evaporator and desuperheated in the condenser. With overcharge too much liquid collects in the condenser and there is also danger of liquid ingestion into the compressor. The TXV can maintain capacity only at

the expense of increased volumetric flow, in the case of undercharge, and increased pressure ratio in both cases. Thus increased compressor power is a symptom of both under- and over-charge. In some cases suction pressure will be too high for the TXV to maintain capacity and loss of capacity will be an additional symptom, albeit not observable by the NILM.

Figure 2 illustrates the increase in compressor power for overcharge. With undercharge, however, power does not quickly settle to a steady value, as shown by the mean P1 transient for each fault level in Figure 3.
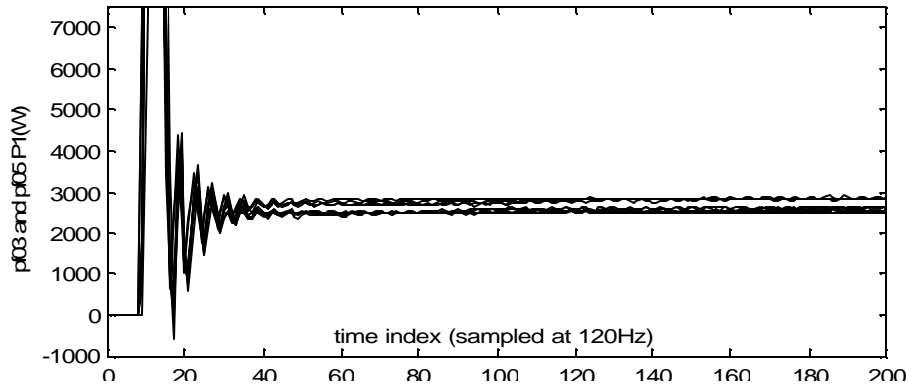

Figure 2. Compressor start transients: lower traces normal, upper with 20% overcharge.
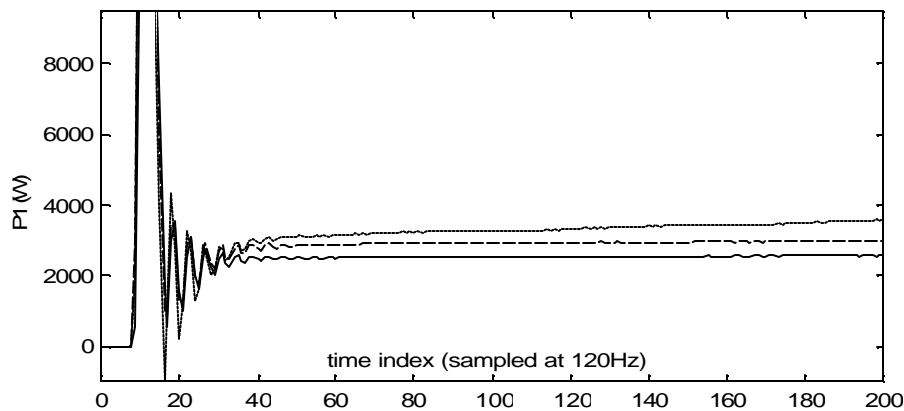

Figure 3. Real power start transients, mean of repetitions for each fault level: normal charge (solid), 20% undercharge (dotted), and 20% overcharge (dashed).

Detection sensitivity and false alarm rate can be estimated from the test samples of mean P1 and Q1. Detection can be based on P, Q, or one of the derived parameters, $R = (P^2 + Q^2)^{1/2}$, or phase angle, $A = \tan^{-1}(P,Q)$. The estimated population distribution for P1, assumed to be Gaussian, is plotted in Figure 4. Sample size is an important factor in detection. One advantage of on-line fault detection is that the parameters for the no-fault condition can be established with relatively high confidence because, in a new RTU, there will usually be a large number of observations, n, before a fault occurs and uncertainty is proportional to $n^{-1/2}$. The vertical dashed line in Figure 4 indicates the sample mean for the no-fault condition. If this mean value were confirmed after many fault-free observations, the probability that the new mean indicated for one of the fault conditions (based on the indicated number of post-fault observations) is truly different from the fault-free mean is given by the area under the distribution minus the area of the tail on the other side of the vertical line. The NILM can be programmed to implement standard tests (Wild and Seber 2000) for change of sample mean given actual sample sizes for the fault-free and post-fault observations that have accumulated at any given time.

We did not assess in these tests the variation of steady-state compressor power that occurs with operating conditions. The observed changes in compressor power alone cannot, therefore, be attributed to a particular fault (overcharge versus undercharge) or distinguished from normal variations in capacity. Discharge-suction pressure difference or condensing and evaporating temperatures could be used to normalize for conditions.
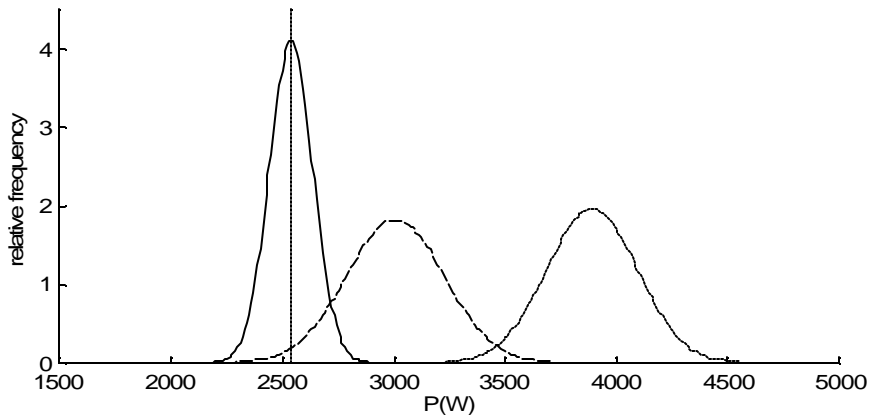
Figure 4. Estimated distributions of steady-state power: normal charge (solid), 20% undercharge (dotted), and 20% overcharge (dashed). Because only a small portion of the tail of the 20% overcharge envelope (centered at 3009W) crosses the no-fault mean (2542W), detection at 20% overcharge will be almost immediate (~10 starts) once the normal-charge mean has been well established. Undercharge is more distinct but settling time is much longer.

3.3 Compressor Back Leakage

Start transients were recorded (4 repetitions) for the compressor/condenser fan with hot bypass and two more start transients were recorded with the bypass closed as shown in Figure 5. The transients with no bypass are the top two. The amplitude difference when the motor is developing peak torque (0.2-0.5s from initial contact) is much greater than the steady-state amplitude difference and, moreover, the shapes of the faulty and fault-free start transients are distinctly different. A simple model, in which evaporator and condenser vapor masses are the only state variables, explains the observed behavior (Armstrong 2004). With a leak fault, condenser pressure builds more slowly until the vapor reaches the saturated condition. Evaporator vapor is already saturated so pressure is initially almost constant, thus initial suction density and flow rate are the same for both cases. With similar mass flow rates, less head translates to lower power initially. At steady state, suction flow rate is higher for the faulty case due to higher evaporator pressure. Despite loss of capacity, with higher flow rate and lower head there is little change in steady state compressor input power.
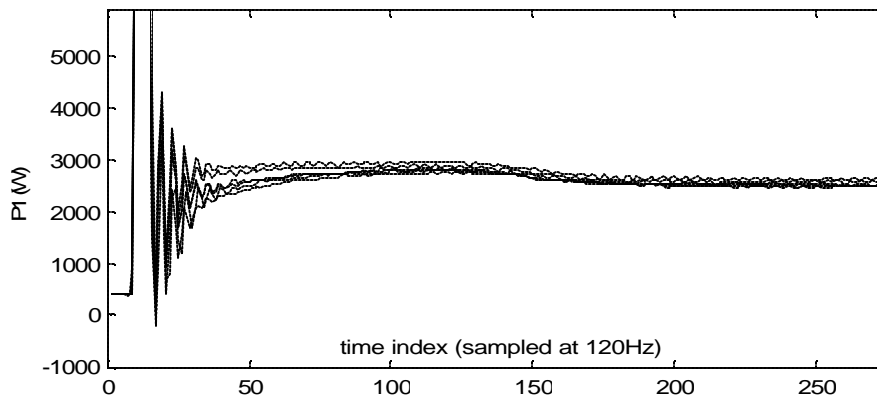

Figure 5. Compressor/condenser active power with bypass leakage (bottom four traces) and without (top two traces).

3.4 Flow Blockage

On the air side, reduced flow (blockage or restriction) is one of the main faults of interest. Condenser fan start transients were measured at three levels of blockage: 0%, 14% and 39% of coil face area. The compressor was locked out and 6-8 repetitions were made at each fault level. Figures 6 and 7 show the mean power, P1, and static-pressure transients for each fault level. Population distributions for P1, derived from the sample mean and variance and assumed to be Gaussian, are plotted in Figure 8. which shows that the lower level of blockage can be detected once the no-blockage mean power is established. Condenser fan power is a good fault detection criterion because it is normally quite constant. Use of temperature-rise based detection, on the other hand, is problematic for the condenser fan blockage fault. Both inlet and outlet sensors are exposed to the elements. The inlet (ambient) temperature sensor in particular is susceptible to radiation, icing, and wet-bulb bias type errors.
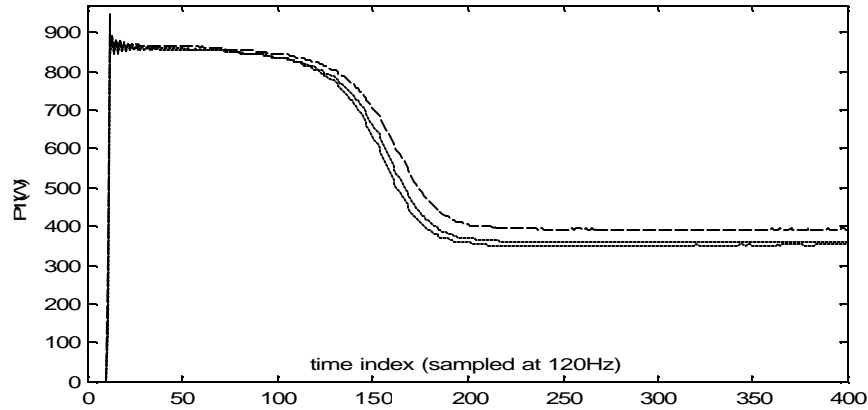
Figure 6. Condenser fan real power start transients, mean of repetitions for each fault level: 0% blockage (solid), 14% blockage (dotted), and 39% blockage (dashed).
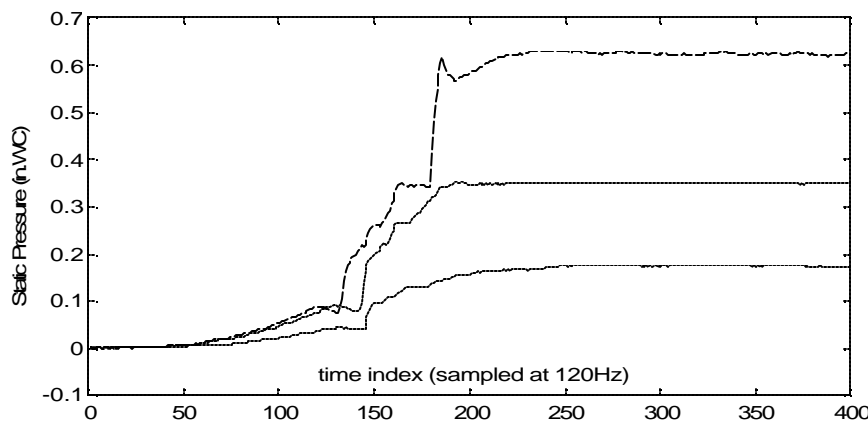

Figure 7. Condenser fan pressure start transients, mean of repetitions for each fault level: 0% blockage (solid), 14% blockage (dotted), and 39% blockage (dashed).
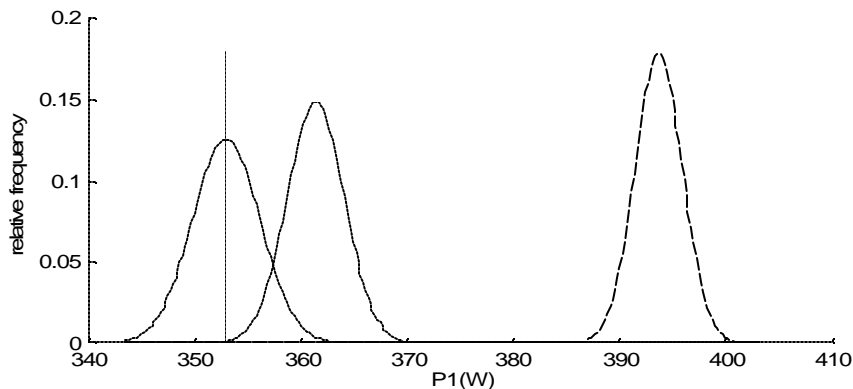

Figure 8. Estimated pdfs of steady power: 0% blockage (solid), 14% blockage (dotted), and 39% blockage (dashed).

Supply-fan start transients were measured with four levels of blockage: 0%, 10%, 50% and 100% of coil face area. Six to eight repetitions were made at each fault level. In contrast to the condenser fan response, supply fan power and reactive power both *decrease* with increasing blockage. This is a consequence of differences in fan curves and the points on those curves that correspond to the respective no-blockage conditions. Moreover, in the case of the supply fan, detection of a blockage is best accomplished by testing the hypothesis that *both* the reactive and real components of steady-state electrical load have deviated from the established no-fault mean values. As shown in Figure 9, it appears that a 10% blockage can be readily detected. However, variations in system resistance resulting from air density changes (Armstrong 1983) upstream or downstream of the fan and changing damper settings may

result in substantial uncertainty in the no-fault means. Further work is needed to understand if the supply fan blockage fault is truly amenable to detection by NILM in the face of such ubiquitous system disturbances.
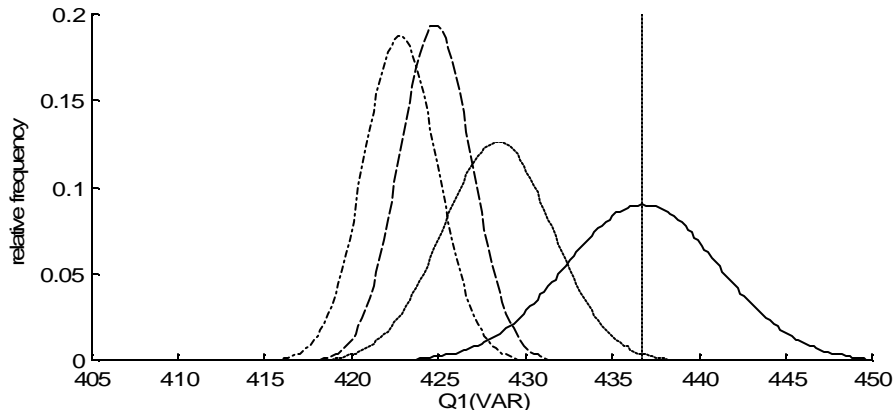

Figure 9. Estimated pdfs of supply fan reactive power: 0% blockage (solid), 10% (…), 50% (.-), 100% (--).

3.5 Load Spectra With Artificially Introduced Imbalance Faults

The condenser fan and supply fan are susceptible to faults that result in impeller or rotor imbalance, vibrations, and associated periodic variations in motor load. Such load variations can be detected by the NILM. Supply fans are typically of the squirrel cage type with direct or belt drive. Imbalance can result from a bent impeller air foil, dirt accumulation or from a foreign object, e.g. piece of filter material, becoming lodged inside the impeller cage. Although not explored here, a bent shaft or damaged sheave will result in periodic motor load variations that can be easily detected and it is likely that serious belt wear can also be detected. Condenser fans are typically of the direct drive axial type with a three- or four-bladed impeller. A cracked blade or blade root is the most common serious fault. A slightly bent blade or shaft or the accretion of dirt will also lead to imbalance and, eventually, to mechanical failure. Early detection is important because the cost to repair collateral damage to a motor or condenser is much higher than the cost to replace a fan impeller.

Periodic load variations may be detected by Fourier decomposition of the power signal, P1. For the condenser fan, the interaction of unbalanced impeller rotation with one of the lower frequency modes in the RTU structure results in a amplitude spectrum peak at 18.4 to 18.7Hz that is very sensitive to fault level as shown in Figure 10. Note that the frequency of this peak drops moderately as imbalance is increased. Figure 11 shows a similar effect of load imbalance for the supply fan. The results for both the supply and condenser fans show that the existence and relative level of imbalance faults can be obtained from signals measured by the standard NILM platform. Appropriate scaling factors for reporting actual fault levels can be determined for a given RTU design by exactly the type of simple test performed here.
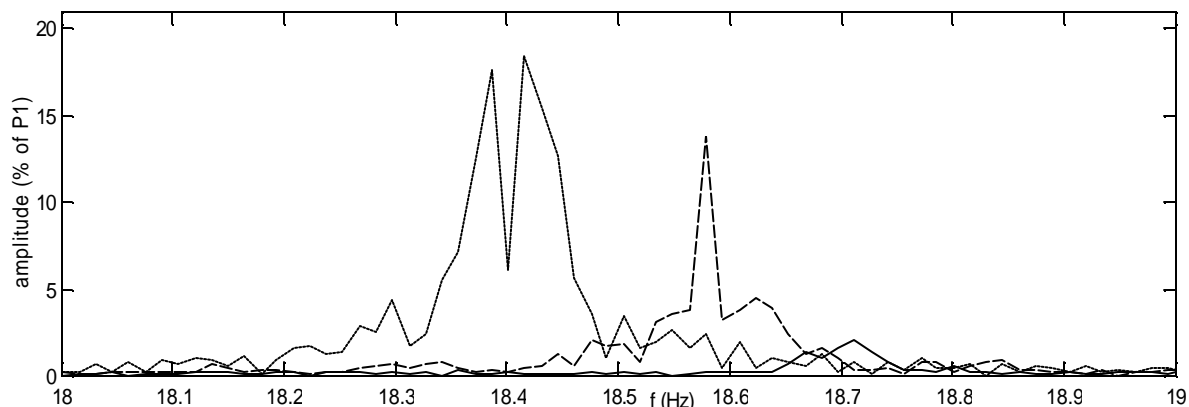

Figure 10. Detail of the FFT (18-19Hz band) of condenser fan power (P1) with 0g (solid), 2.6g (dashed) and 5.3g (dotted) imbalance fault levels.
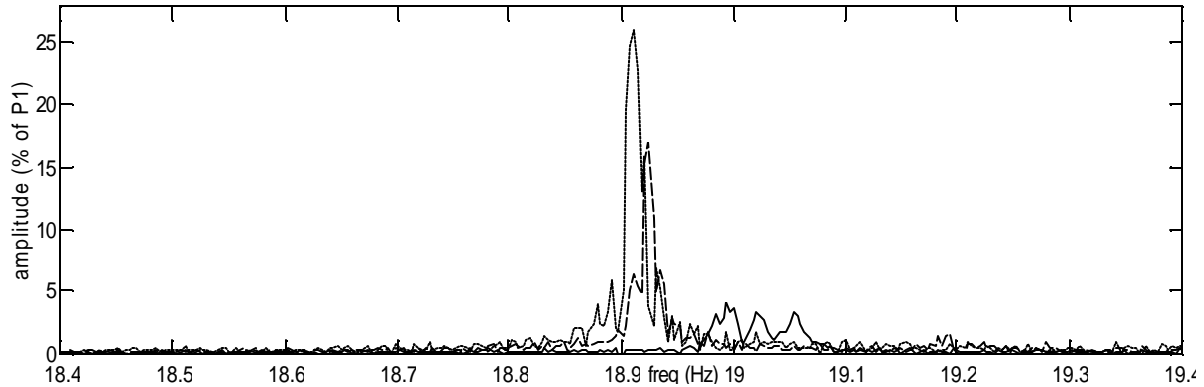
Figure 11. Detail of the FFT (18.4-19.4Hz band) of supply fan power (P1) with 0g (solid), 8g (dashed) and 16g (dotted) imbalance fault levels.

3.6 Compressor Liquid Ingestion

Compressor damage by liquid ingestion is likely to be preceded by one or more incidents in which small, relatively inconsequential, amounts of liquid enter the machine[3]. The NILM's ability to detect flooded starts and liquid slugging was tested in the lab by introducing a known, repeatable mass of liquid at the suction port of a small semi-hermetic compressor. The mean of five wet (1 cc oil) and five dry start transients are shown in Figure 12. While the difference is visually small, the shape of the difference, Figure 13, shows that reliable detection is possible, with power peaks occurring only during the compression stroke; a similar shape was found for the injection of 3 cc of liquid R-30 refrigerant.
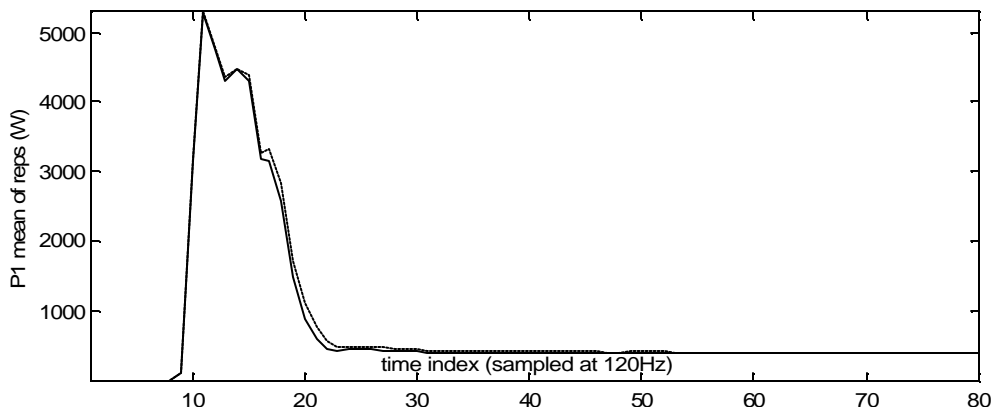

Figure 12. Mean of repetitions with no fault (solid) and 1.0 cc liquid ingestion (dotted).
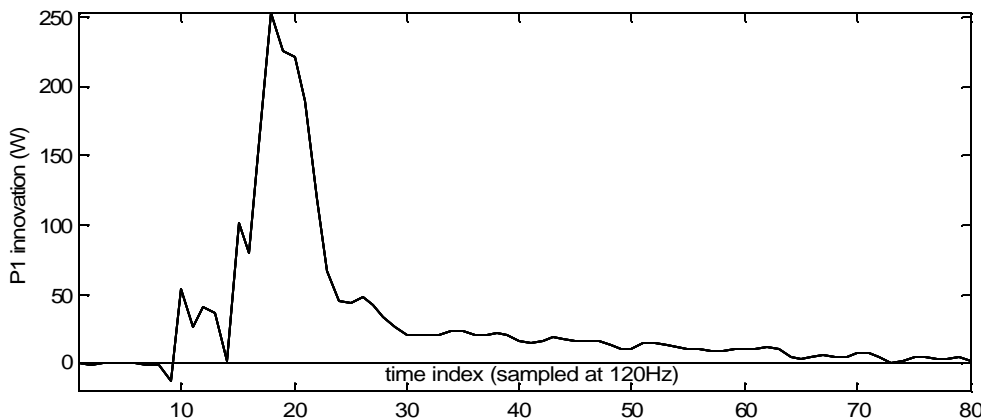

Figure 13. Mean deviation of P1 for starts with 1.0 cc liquid from P1 for fault free starts.

---

[3] An amount of liquid that fills the clearance volume, about 2% of displacement, can cause damage.

Another type of liquid ingestion fault involves liquid entering the compressor during steady operation. This might be caused by an intermittent TXV fault. To observe this effect, equal doses of oil were injected, at the rate of about one injection every 20s, during steady operation. A series of five events was observed with 1.0 cc oil injected at the suction port for each event. The P1 transients observed in the test are plotted (superimposed) in Figure 14. Compressor power increases briefly (by about 15W (2.5%) for 300ms) and then returns gradually to normal. Note that a reciprocating compressor presents a cyclic load component corresponding to shaft speed because more torque is required during suction and compression than when the crank is taking the pistons through their top and bottom positions. The shaft speed cycle interacts with line frequency to produce strong beats, evident in Figure 14 at 3.6Hz.
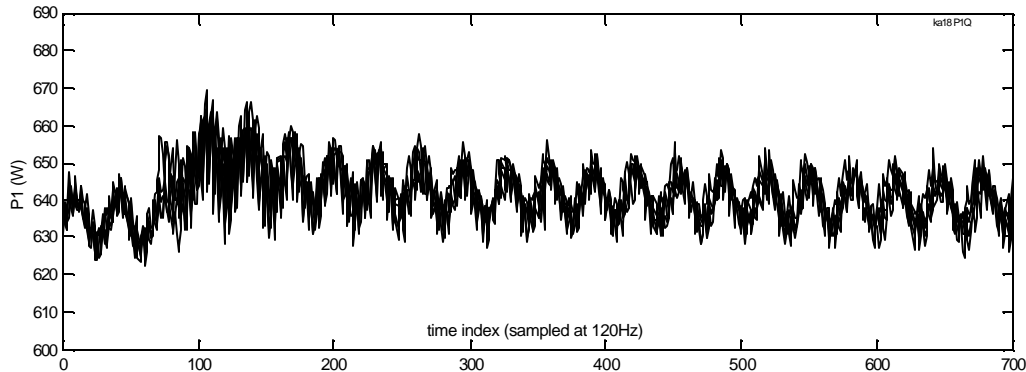

Figure 14. Real power during steady run liquid ingestion, five repetitions.

The effect on P1 of ingesting non-damaging amounts (<5cc) of liquid is small, making reliable detection difficult. There are three aspects of the difficulty: 1) small magnitude of the change relative to normal variations in P1, 2) lack of abrupt transient features, and 3) lack of a distinct transient shape. There is a further difficulty, not apparent in the 1-10s time frames plotted above, that the dc component of P1 varies gradually with refrigeration load, ambient temperature, and stator temperature. To address these difficulties, we applied a generic (5th-order autoregressive with trend term) adaptive model of the process to provide not only k-step-ahead predictions, but also estimates of the variances of prediction errors. Together these numbers may be used to reduce detection to an adaptive scalar threshold test based on the norm of squared innovations, inversely weighted by the k-step-ahead prediction variances. A further important function of the adaptive process model is in isolating a new start transient from the background signal that is the sum of all loads that are active when the new load is switched on.

4. SUMMARY AND DISCUSSION

A NILM FDD implementation requires only current and voltage sensors at the RTU feed, all located safely in the electrical box. A single-phase NILM requires one current sensor and one voltage sensor, while a three-phase NILM requires two of each sensor. There may be a niche for a NILM with one current and three voltage sensors so that phase imbalance or phase loss can be immediately detected. The single-phase NILM can be implemented in a low cost 150 MHz PC-on-a-chip with a two channel A/D converter, with an incremental RTU manufacturing cost as low as $200. Integration with RTU controls is a natural extension which reduces the incremental cost of FDD capability and may be especially attractive for high SEER designs with variable-speed fans or compressors.

Air-side blockage faults can be detected by a shift in steady state power and, to some extent, by changes in start transient shape. Because change magnitudes and directions are related to blockage magnitude via the interaction of fan curve, air-side flow-pressure curve, motor torque curve and no-fault operating point, diagnosis requires more information than that needed for detection, e.g. addition of static pressure.

Short cycling can be detected in the obvious way, by logging time between start transients. The advantage over detection by a temperature-sensor-based FDD system is that very short—even incomplete—start transients are detected. This is important because just a few inrush current events in quick succession will raise stator winding temperature to the point of insulation damage. A second and complementary detection method relies on the shape of individual start transients being sensitive to residual head. A time-stamp and the thermal conditions at the time of each short-cycle occurrence can be saved to aid in diagnosing a root cause.

Refrigerant charge faults result in elevated head pressures which cause higher steady-state compressor loads. Detection of overcharge requires normalizing compressor load over the range of thermal operating conditions. Detection of undercharge is possible based only on the distinct shape of its start transient.
The refrigerant vapor bypass fault has a distinct effect on the start transient shape: the change of magnitude in the latter half of the transient is two to five times the change in steady state power.

Liquid ingestion results in a change in start-transient shape that is small in magnitude but has distinct compression-stroke features. The shapes of liquid-ingestion transients during steady operation always result in increased power of 0.1-1s duration and this increase appears clearly as positive deviations from k-step-ahead forecasts. Conditions recorded at the time of occurrence can be saved to aid in diagnosing a root cause.

Shaft harmonics observations with no fault indicate that direct drive fan harmonics are not as obvious as belt driven shaft harmonics (Lee 2003) but are still potentially useful for load identification. The results of tests using small weights to unbalance the impellers indicate that the NILM can identify degradation of impeller balance well before catastrophic failure and associated additional repair costs are incurred.

The NILM uses five generic detection methods. *Current and voltage* imbalance (or complete loss of phase) are detected by simple ratio and threshold tests. A *change-of-mean* results from a change in steady state mechanical load that is detected as a change in electrical power, P1, with corresponding changes in reactive and apparent power and a corresponding change in power factor. *Start transients* are identified by pattern matching. The motor associated with a measured transient is first identified using a generous confidence interval and a tighter confidence interval is then applied to detect a possible fault. *Event sequence* analysis compares the timing and sequence of motor state (on, off) changes to the sequences expected in response to given controller commands. The NILM's very high time resolution of motor start and stop detection and ability to log the sequences for playback by a technician are put to good use here. The *amplitude spectrum* of power, P1, is used to detect shaft, coupling, rotor, impeller, and belt-drive faults.

The suite of faults that are best detected by the NILM complements, to large extent, the faults that are best detected by temperature-based FDD systems. Faults that are primarily electrical or electro-mechanical are difficult to detect by thermal measurements but can be detected by the NILM using the methods indicated in Table 1. The NILM can also play a role in detecting many of the more interesting non-electrical faults as summarized in Table 2. A comprehensive FDD system could employ an extension of the models developed by Rossi (1997) and Breuker (1998), which currently use return air and ambient air conditions as inputs, by adding compressor power as an input.

Table 1. Summary of electrical and electro-mechanical RTU faults detectable by the NILM alone.

Fault	NILM Method
Loss of phase	Current and Voltage
Locked rotor	Start transient
Slow starting motor	Start transient
Unbalanced voltage	Voltage
Short cycling	Event sequence
Motor disconnect/failure to start	Event sequence
Incorrect control sequence	Event sequence
Contactor (improper contact closure)	Phase current interruption transient
Fan rotor faults that result in imbalance	Amplitude spectrum in steady operation
Compressor mechanical faults (not tested)	Amplitude spectrum in steady operation

Table 2. Summary of non-electrical faults. Some of these can only be detected by the thermal measurements and some can only be detected by the NILM, but detection of most can benefit by having both types of measurements.

	Fault	NILM Method	7T[1]	10T[1]
1	Refrigerant leakage, undercharge, or overcharge	Change of mean	∨	∨
2	Liquid line restriction		∨	∨
3	Loss of volumetric efficiency (leaky valves, seals)	Start transient	[2]	∨
4	Fouled condenser coil	Change of mean	∨	∨
5	Dirty supply air filter	Change of mean [3]	∨	∨
6	Liquid ingestion	Anomalous transient		
7	Vapor line restriction	[4]		
8	Non-condensable gas	[4]		
9	COP degradation (root cause: 1, 2, 3, 4, 5, 7 or 8)	[5]	[6]	[6]

[1] 7T FDD measures Twb, Tamb, Tevp, Tsh, Thg, Tcnd, and Tsc; 10T FDD also measures Tra, ?Tcndair, and ?Tevpair (Breuker 1998).
[2] low sensitivity
[3] system flow-pressure-temperature model may be needed for reliable detection
[4] not tested
[5] with addition of refrigerant flow (or comnpressor map) and head pressure
[6] with addition of air-side flow and RH

ACKNOWLEDGMENT

REFERENCES

Armstrong, P.R., 1983. Instrumentation of Solar Heating and Cooling Systems at CSU, Invited paper, Proc. 2nd Workshop on Performance Monitoring, FSEC, Cape Canaveral.

Armstrong, P.R., 2004. Model Identification with Applications to Building Control and Fault Detection, Ph.D. thesis, Massachusetts Institute of Technology.

Breuker, M.S. and J.E. Braun, 1998a. Common faults and their impacts for rooftop airconditioners, *HVAC&R Research*, 4(3) pp.303-318.

Breuker, M.S. and J.E. Braun. 1998b. Evaluating the performance of a fault detection and diagnostic system for vapor compression equipment. *HVAC&R Research*, 4(4) 401-425.

Katipamula, S. and S. Gaines, 2003. Characterization of Building Controls and Energy Efficiency Options Using Commercial Building Energy Consumption Survey, PNWD-3247.

Laughman, C.R., *et al*, 2003. Power Signature Analysis, *IEEE Power and Energy*, March 2003.

Lee, D.K. 2003. Electric Load Information System Based on Non-Intrusive Power Monitoring, Ph.D. thesis, MIT.

Leeb, S. B. 1992. A Conjoint Pattern Recognition Approach to Non-Intrusive Load Monitoring. Ph.D. thesis, MIT.

Rossi, T. and J. Braun, 1993. "Classification of fault detection and diagnostic methods," *Building Optimization and Fault Diagnosis Concepts* Int'l Energy Agency Annex 25

Rossi, T. and J. E. Braun. 1997. A statistical, rule-based fault detection and diagnostic method for vapor compression air conditioners. *HVAC&R Research* 3(1), pp.19-37.

Shaw, S. R., C. B. Abler, R. F. Lepard, D. Luo, S. B. Leeb, and L. K. Norford, 1998. "Instrumentation for high performance nonintrusive electrical load monitoring," ASME J Solar Energy Engineering, vol. 120, pp. 224-229.

Shaw, S.R., and S.B. Leeb, 1999. Identification of Induction Motor Parameters from Transient Stator Current Measurements, *IEEE Trans. Industrial Electronics*, 46(1) pp.139-149.

Shaw, S.R., 2000. System Identification Techniques and Modeling for Nonintrusive Load Diagnostics, Ph.D. thesis, Massachusetts Institute of Technology.

Stouppe, D.E. and T.Y Lau, 1989. "Air conditioning and refrigeration equipment failures," National Engineer, 9/89.

Wild, C.J. and G.A.F.Seber, 2000. Chance Encounters: A First Course in Data Analysis and Inference, Wiley.